KSCE Journal of Civil Engineering
Vol. 7, No. 3 / May 2003
pp. 225~231

*Construction Management*

# Rapid Geometric Modeling for Construction Automation

**By Yong-Kwon Cho* and Soon-Wook Kwon****

## Abstract

Most automated and semi-automated construction tasks require real-time information about the local workspace in the form of 3D geometric models so that on-site decisions can be made quickly and safely. This paper describes and demonstrates a new rapid, local area, geometric data extraction and 3D visualization method for unstructured construction workspaces that combines human perception, simple sensors, and descriptive CAD models. This paper also presents algorithms to fit objects to sparse point clouds of measured data in a construction scene, that significantly decrease data acquisition time, and computational and modeling time.

Keywords: *construction automation, 3D modeling, laser range finder, least squares method*

## 1. Introduction

Laser range scanner has been widely used to obtain 3D range data for construction site scenes. The uses of laser range scanners in the construction industry include: (1) generating 3D as-built model, (2) tracking terrain changes due to excavation, (3) site inspection, (4) aerial surveying, and (5) process simulation and operator training.

Using automated or semi-automated equipment on a large construction site requires rapid recognition and accurate measurement of objects in the workspace so that timely on-site decisions can be made.

Rapid local model related research such as the Autonomous Loading System (ALS) was conducted at the Robotics Institute at Carnegie Mellon University (Stentz *et al.* 1998). This system uses two laser range scanners whose purpose is to recognize and localize the truck, detect obstacles, and measure the soil face. One of the disadvantages in ALS is that whenever a new truck arrives for loading, the ALS must repeat the computing process of matching model-to-scene. This results in decreased efficiency because the most important issue of ALS is to ascertain object location, not to recognize the object.

In previous attempts to solve the problem of rapid recognition and accurate measurement of objects in the workspace, most researchers have focused on building comprehensive 3D models of the workspace derived from a combination of design data and from highly computationally intensive interpretation of dense clouds which have hundreds of thousands points at a scene and position data (Bary *et al.* 1997, Stentz *et al.* 1998, and Witzgall *et al.* 2001). Low accuracy in extracting objects from dense clouds is an additional limitation of full range scanning methods. Recent research indicates that graphic workspace modeling and graphical equipment control technologies can in fact improve equipment control significantly in several construction automation applications such as heavy lifting, earth moving, material handling, and infrastructure repair and maintenance (Haas 1995). However, comprehensive local area modeling based on fusion of dense point clouds is impractical and unnecessary in practice in the near future (Cho 2002).

By strategically incorporating human assistance, which can simplify and accelerate geometrical data acquisition of real-world objects considerably, the ability to extract models of real world objects in a construction workspace for equipment operations from only a limited number of scanned points is a significant advantage of this approach over full range scanning methods that require computationally intensive range data processing.

This paper presents a new method for rapid geometric

*Corresponding Author, Assistant Professor, Dept. of Industrial Studies, University of Wisconsin, Platteville, WI 53818. (E-mail: choyo@uwplatt.edu)
**Graduate Research Assistant, Dept. of Civil Eng., The University of Texas, Austin, TX 78712 (E-mail: swkwon@mail.utexas.edu)

The manuscript for this paper was submitted for review on January 2, 2003.

modeling and visualization of a local areas based on spatial information about objects obtained using simple sensors (such as a single-axis laser rangefinder and a video camera) for better planning and control of automated construction equipment operations in unstructured workspaces.

## 2. Rapid Modeling Methods

In this research, current approaches to workspace modeling include: (1) human assisted selected-points based local area sensing and (2) analysis of sparse range point clouds, using such methods of least-square-fits to planar and curved surfaces. The results of their applications are presented in the following sections.

### 2.1. Human Assisted Selected-Points Based Local Area Sensing

Since most target objects are known and man-made, they can be described as a generic set of parametrically defined graphical objects in a computer database (Cho 2002). Such a library of pre-stored models (related to facility design elements), with manual guidance, can provide graphic representations of forms that can be matched and fitted to sensed data from 3D position sensors deployed in the work environment. The matching and fitting process is equivalent to setting the values of the object parameters that define it.

#### 2.1.1. Boundary Representation of Objects

Faces, edges and vertices are the basic geometric elements required for a boundary representation of a solid object. As long as the Cartesian coordinates of a certain number of vertices, or points on the edges or on the faces of the object, are identified, position and orientation of most solid objects can be determined. The number of vertices or points on the edge or a surface depends on the geometric and topological features of the solid object.

Primitives that could be used to represent or construct typical construction material such as pipes and I-beams were examined. A single-axis laser range finder was used to obtain the minimum required points with regard to an objects position and orientation. Given the lack of precise control of the measuring device and hand-eye coordination of a typical operator, acquiring these points is sometimes difficult to implement in practice. Practical means to deal with this issue are partially addressed by this research but are more fully addressed in subsequent follow-up research (analysis of sparse range point clouds).

(1) Box (Cuboid)

A box can be used for fitting and matching structural objects such as columns, box-beams and walls and finishing objects. A box which has been unambiguously identified can be easily located with respect to its position and location as long as the positions of three vertices can be measured (Fig. 1). If the box is ambiguous and parametrically defined, a fourth point is required to determine its depth.

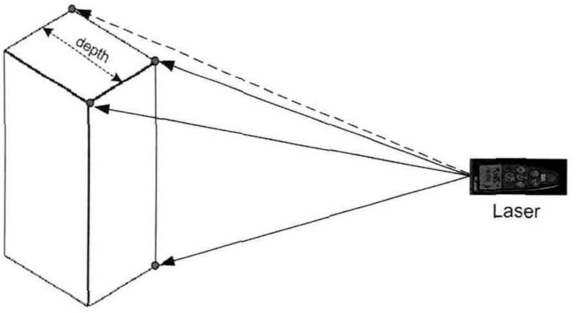


Fig. 1. Vertices Measuring for a Box Modeling

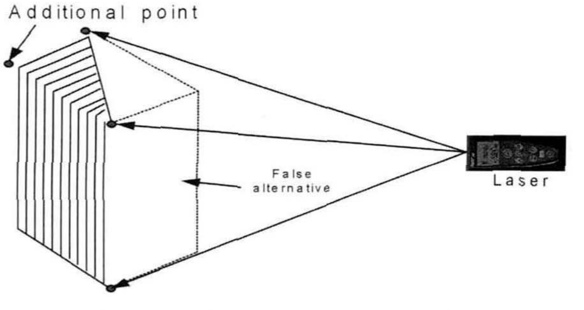


Fig. 2. Vertices Measuring for a Prism Modeling

(2) Prism

Three vertices are required to locate a prism. However, sometimes three points may induce a directional confusion in the boundary for the operator. An additional point can prevent this problem (Fig. 2).

(3) Cylinder

Cylinders can be used to fit and match chemical pipes, ventilation pipes, and concrete piles. Although the operator can see the vertices on silhouette edges that indicate the diameter of the cylinder, in practice, a laser can not measure the outer most points on the round edge because it reflects the footprint of the laser. In addition, the footprint of the laser becomes highly diffused because of the low angle of incidence at which it illuminates the cylinder edge. Thus, unlike a box or a prism, a cylinder requires more than three points. Based on the fact that there is only one circle that passes through three points, the triangle created by the three points determines the size and position of the circular face

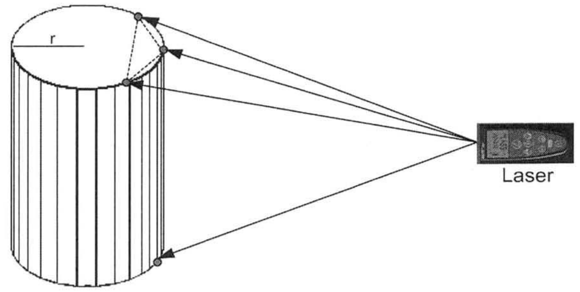


Fig. 3. Edge Measuring for a Cylinder Modeling

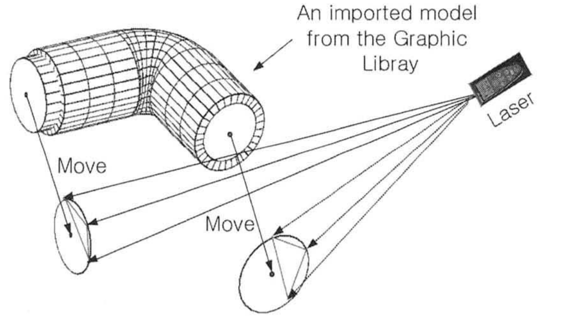


Fig. 4. A Pipe Connector Modeling Process

of the cylinder A fourth point on the other edge of the cylinder will determine the direction and length of the cylinder, as shown in Fig. 3.

(4) Pipe Connector

The pipe connector was formed by three cylinders (two 9" and one 8" cylinders) and a quadrant of a torus. As long as two circles are defined with six points on the boundary edge, a pre-designed pipe connector can be easily located (Fig. 4).

2.1.2. Trench Modeling

A small trench was created at the laboratory's outdoor facilities, and the laser/camera system was used to obtain geometric data for the trench, a pipe connection of two aluminum pipes and a pipe connector based on the aforementioned well-known geometry laws. The range of measurement of the laser range finder is 100 m with accuracy of ±3 mm. The step size of the tele-operated pan and tilt unit, which controls the laser range finder, is of high resolution (0.0128571°/step) and its maximum speed is a little over 60°/second.

The purpose of this graphical modeling experiment for a trench site was to demonstrate the potential of this method to keep people out of a trench, to provide a safety boundary representation of a trench with a form of non-parametric model, and to provide the operator with precise spatial information that can potentially improve equipment control for high precision pipe placing and connecting tasks in a trench.

Especially, the safety boundary representation of the trench can eliminate interference between the equipment and the trench walls during operation. Thus, instead of describing the detailed topography of the trench, seven points located slightly inside its walls were measured to represent this safety boundary (Fig. 5).

Like the pipe connector, six points were measured to


Fig. 5. Safety Boundary Measurement for a Trench

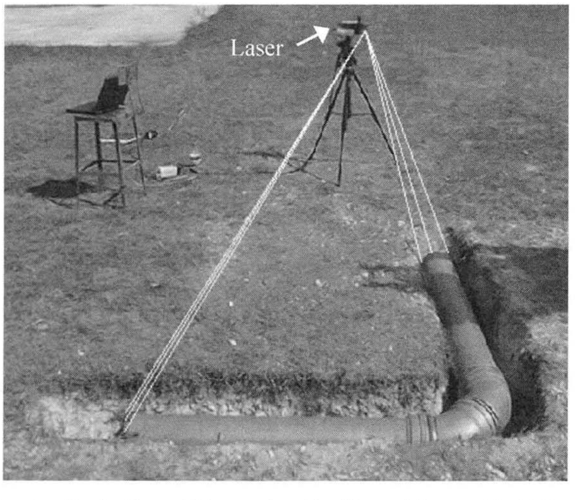


Fig. 6. Illustration of Measuring Position of Assembled Pipes with a Laser Range Finder

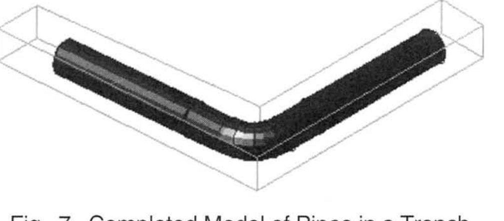

Fig. 7. Completed Model of Pipes in a Trench

identify the position and orientation of the assembled pipes (Fig. 6). Then, pre-designed assembled pipes were imported to the scene for the fitting and matching process based on the measured surface data. Fig. 7 shows the completed as-built design of pipes in the trench.

## 2.2. Analysis of Sparse Range Point Clouds

This section presents algorithms that accurately fit and match objects, with regard to location and orientation, to sparse point clouds in a construction scene.

The single-axis laser range finder was also used to get the sparse point clouds from objects. The modeling process involves the following functions:

1. Select object for scanning (by operator)
2. Acquire sparse point cloud data in the form of range images
3. Convert range data into xyz coordinates
4. Analyze the features of each surface of the object
5. Match all of the object surfaces with the model's surfaces using matching algorithms
6. Fit the object into the point cloud using fitting algorithm

The following fitting and matching algorithms were developed for each primitive:

1. Cuboid algorithm
2. Cylindrical object algorithm

Since cuboid and cylindrical shapes of primitives consist of 6 planar surfaces (cuboid), and two planar surfaces and one curved surface (cylinder), the algorithms were developed as a surface based fitting and matching method. Algorithm development and revisions were based on lab experiments.

### 2.2.1. Cuboid Algorithm

This section describes how to fit a sparse points cloud to a cuboids surfaces using the *k*-nearest neighbors and the least squares methods.

#### 2.2.1.1. Point Segmentation Using K-Nearest Neighbors Method

To find the nearest points for all measured points on a cuboid, a k-nearest neighbor algorithm was used. The algorithm finds the nearest two points by computing all the distances from a scanned point to all other points (Duda *et al.* 2001). After determining two nearest neighbors for each scanned point, a group of three-point sets was found. Then, a normal vector for each three-point set was computed. By analyzing normal vectors, the scanned points were segmented by each cuboid surface.

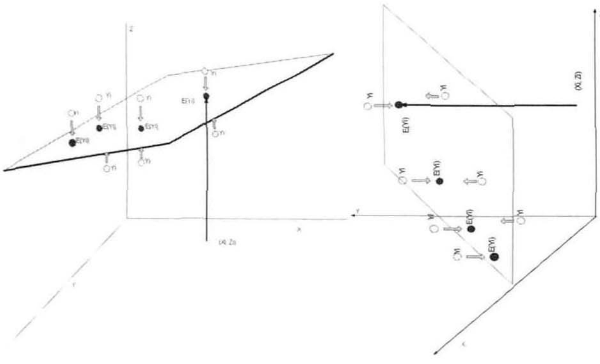

Fig. 8. Surface Optimization

#### 2.2.1.2. Plane Optimization Using the Least Squares Fitting Method

The least squares method (Duran *et al.* 1973) was used for the best-planar fit of point sets on each surface of the cuboid after segmentation was applied.

Since in a planar regression, $Y$ is to be regressed on two independent variables $X$ and $Z$, a relationship, where both $X$ and $Z$, are calculated as deviations from their means, was used:

$$E(Y_i) = \alpha + \beta_i \cdot X_i + \gamma \cdot Z_i \tag{1}$$

For any given combination of $X_i$ and $Z_i$ the expected yield $E(Yi)$ is a point directly above the plane, shown as a hollow dot in Fig. 8. The actual value of the component $Yi$ of an observed point is somewhat greater than its expected value and is shown as a solid dot lying on the plane. The difference between the observed and expected values of $Y_i$ is shown by the error term $e_i$ and thus the observed value $Y_i$ is expressed as its expected value plus the error term $e_i$:

$$Y_i = \alpha + \beta_i \cdot X_i + \gamma \cdot Z - e_i \tag{2}$$

While moving along the $x$-direction, $\beta_i$ is interpreted as the slope of the plane. In the same way $\gamma$ is the subsidiary effect of $z$. To minimize the error sum of the squares a coefficient is used:

$$\sum_{i=1}^{N}(Y_i - \hat{Y})^2 = \sum_{i=1}^{N}(Y_i - \hat{\alpha} + \hat{\beta} \cdot X_i + \hat{\gamma} \cdot Z_i)^2 \tag{3}$$

Taking the partial derivatives of the above expression with respect to $\hat{\alpha}$, $\hat{\beta}$ and $\hat{\gamma}$, and setting them to zero, finally alpha, beta, gamma are found. Using this expression, the three optimized surfaces of the cuboid are computed (Fig. 8). After segmenting all scanned points by the three surfaces of the cuboid, the points were projected onto the optimized surface to compute dimensions.

2.2.1.3. Determining Intersecting Edges and Computing Dimensions

The three surface planes of the cuboid, from which range data were received, intersect at a point, and each two planes intersect at a line. The intersection of the two planes of the cuboid was found by solving the two linear equations representing the planes. After applying this for all three surfaces of the cuboid, the three edges of the cuboid were determined and matched. A vertex of the cuboid was also determined. Figs. 9 and 10 show the results of point segmentation, and matching vertex process.

Once the three edges of the cuboid were defined, the dimensions of the cuboid were determined as follows: By computing the distances of all measured points on each surface to each one of the already defined edges of the same surface, the furthest point from each edge was found. The distances of the furthest points on the surfaces from the three intersecting edges represent the dimensions of the cuboid.

Fig. 11 shows a fitted and matched model of an object

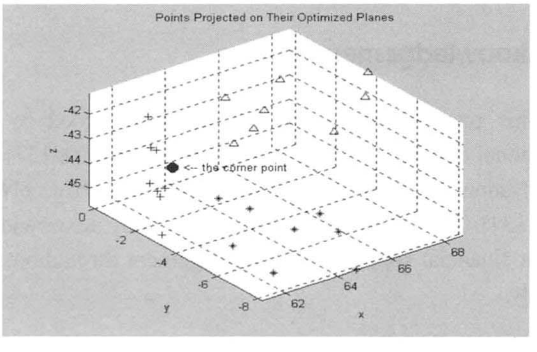


Fig. 9. Matching Points and Segmentation

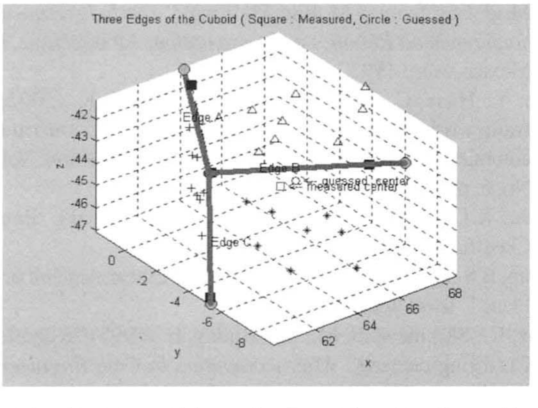


Fig. 10. Three Edges of a Cuboid and its Centroid

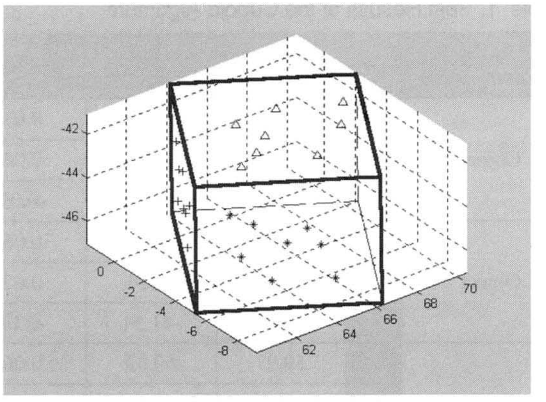

Fig. 11. Fitted and Matched Cuboid

after the application of the cuboid algorithm.

2.2.2. Cylindrical Object Algorithm

Four parameters are required for fitting and matching a solid cylinder: a scalar radius $r$; an axis vector, $a$; a center point to determine the axis vector, $c=(X_c, Y_c, Z_c)$ and a set of scanned points $g=\{(X_i, Y_i, Z_i)\}$ to find out the boundary of the cylinder. To determine the normal vector, the "k-nearest neighbors method" was used. Then, by analyzing normals, the scanned points were segmented by surface (planar or curved). Subsequently, by projecting all points on the curved surface onto the planar surface, parameters $r$ and $c$ were estimated. The least squares method was also used to optimize the curved surface. The radius of the cylinder was found as the distance from the center of the circle to any point on the optimized curve. Projected points on the planar surface are considered end points of different chords in the circle and used to estimate its center $\hat{c}$. An initial estimate of the radius, $\hat{r}$, is found by $\hat{r} = mean(|\hat{c}-k'|)$ ($k'$ = {the points on the optimized curve of planar surface}).

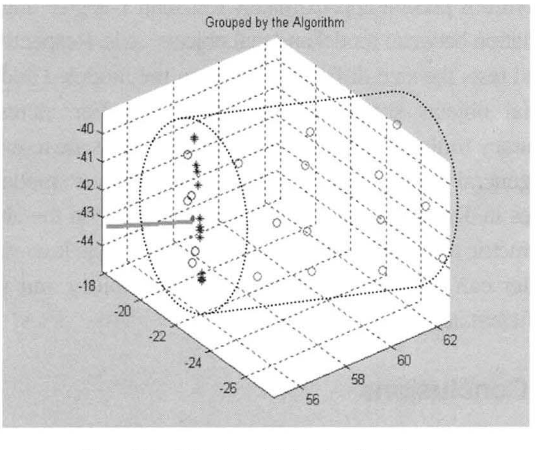


Fig. 12. Fitted and Matched Cylinder

Table 1. Test Results of the Cuboid Algorithm

| Matching Point (vertex) | | Modeled Object | Actual Object | Deviation |
|---|---|---|---|---|
| Object 1 | x | 57.75 | 57.82 | 0.07 |
| | y | 11.7 | 11.73 | 0.04 |
| | z | -35.45 | -35.46 | -0.02 |
| Object 2 | x | 59.98 | 60.04 | 0.06 |
| | y | -5.2 | -5.14 | 0.07 |
| | z | -41.37 | -41.54 | -0.17 |
| Object 3 | x | 59.97 | 60.03 | 0.06 |
| | y | -5.18 | -5.11 | 0.07 |
| | z | -41.35 | -41.49 | -0.14 |
| Object 4 | x | 59.92 | 60.03 | 0.11 |
| | y | -5.17 | -5.11 | 0.06 |
| | z | -41.21 | -41.62 | -0.411 |
| Angular deviation between edges | Edge A | | | 1.089 |
| | Edge B | | | 1.824 |
| | Edge C | | | 0.927 |
| Measuring + Computing time | pts | Measuring (sec.) | Computing (sec.) | Total (sec.) |
| Object 1 | 15 | 30 | 5.87 | 35.87 |
| Object 2 | 20 | 50 | 5.66 | 55.66 |
| Object 3 | 25 | 60 | 6.48 | 66.48 |
| Object 4 | 30 | 80 | 5.6 | 85.6 |

Then the final values of a, c, and r are found by applying the least squares method to all scanned data (Fig. 12).

2.2.3. Experimental Results of Sparse Range Point Clouds Method

Table 1 shows an example of experimental results of a cuboid fitting and matching process. The test results of the algorithms present approximately less than 1-degree angular deviation between model and real objects' axis. Respectively in all tests the size difference between the modeled and the actual objects surfaces is less than 5%. For increased accuracy further modifications of the algorithms are required. In general low deviation values, and the low modeling times in Table 1 indicate that a system based on the above geometric algorithms and a human-guided simple laser range finder can model construction objects rapidly and with sufficient accuracy.

## 3. Conclusions

A new rapid local area workspace modeling method has been developed by combining human perception, pre-stored CAD objects, and use of simple sensors such as single-axis laser rangefinders and remote video cameras. Two approaches were conducted: (1) human assisted selected-points based local area sensing and (2) analysis of sparse range point clouds, using such methods of least-square-fits to planar and curved surfaces.

The fitting and matching algorithms discussed in this paper, are an integral part of a method that involves several other functions such as: human object recognition, collecting of range information, grouping of scanned points, and computing dimensions to final fitting and matching. A basic feature of the method is that it takes advantage of human cognitive ability to recognize and classify objects in the workspace; that is a human operator initiates scanning, recognizes objects, and controls the system for data acquisition. In addition fitted and matched objects are verified by the operator and then inserted into the workspace model.

The rapid geometry modeling method can significantly reduce modeling time while potentially increasing modeling accuracy in terms of volume, position, and orientation. Potential impact of this research includes safer and more efficient operations with computer-assisted construction and maintenance equipment.

## Acknowledgements

This paper is based on the research funded by the National Science Foundation (Grant#: CMS-0000137) and the National Institute Standard and Technology (Project NBR: NA1341-02-W-0742). The authors gratefully acknowledge their financial support and encouragement throughout this study.

## References

Barry, R., Jones, J., Little, C., and Wilson, C. (1997) "Rapid World Modeling from a Mobile Platform." *IEEE-International conference on Robotics and Automation*, Albuquerque, New Mexico, April 1997.

Cho, Y., Haas, C., Sreenivasan, S., and Liapi, K. (2002) "A framework for rapid local area modeling for construction automation." *Journal of Automation in Construction*, Vol. 11, No. 6, pp. 629-641.

Duda, R.O., Hart, P.E., and Stork, D.G. (2001) "Pattern Classification." Wiley Inter-Science.

Duran, B.S. and Amir-Moez, A.R. (1973) "Linear Algebra of The Plane." Texas Tech University.

Haas, C., Skibniewski, M., and Budny, E. (1995) "Robotics in Civil Engineering." *Microcomputers in Civil Engineering*, October, pp. 371-381.

Stentz, A., Bares, J., Singh, S., and Rowe, P. (1998) "A Robotic

Excavator for Autonomous Truck Loading." *Proceedings IEEE/RSJ International Conference on Intelligent Robotic Systems*, October, Victoria, B.C., Canada.
Witzgall, C. and Cheok, G. (2001) "Registering 3D Point Clouds: An Experimental Evaluation." NISTIR 6743, National Institute of Standards and Technology, Gaithersburg, MD, May.